Science of the Total Environment 838 (2022) 156494

Contents lists available at ScienceDirect

Science of the Total Environment

journal homepage: www.elsevier.com/locate/scitotenv

Acid-mediated hydrothermal treatment of sewage sludge for nutrient recovery

Andres Sarrion [a,*], Angeles de la Rubia [a], Charles Coronella [b], Angel F. Mohedano [a], Elena Diaz [a]

[a] Department of Chemical Engineering, Faculty of Sciences, Universidad Autónoma de Madrid, Campus de Cantoblanco, 28049 Madrid, Spain
[b] Chemical and Materials Engineering Dept., University of Nevada, Reno, 1664 N. Virginia St., NV, United States

HIGHLIGHTS

- Acid-mediated hydrothermal treatment of sewage sludge for nutrient recovery
- HCl-mediated HTC at 230 °C remarkably increased P and N recovery in process water.
- Phosphorus extraction from sewage sludge was optimized at 15 min HCl-mediated HTC.
- Acid-mediated HTC improved hydrochar characteristics as a solid biofuel.

GRAPHICAL ABSTRACT

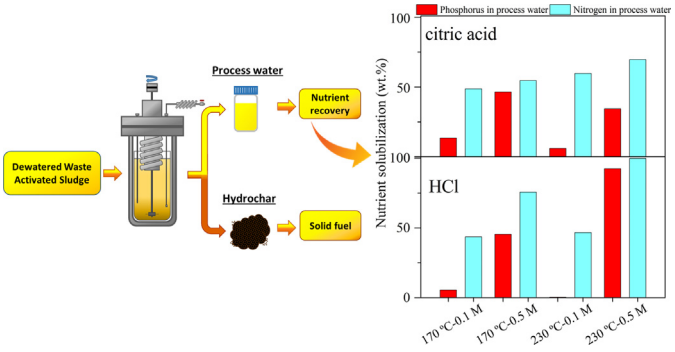

ARTICLE INFO

Editor: Daniel CW Tsang

Keywords:
Biofuel
Biomass treatment
Hydrothermal carbonization
Nutrients and energy recovery
Waste-activated sludge

ABSTRACT

Hydrothermal carbonization allows material valorization and energy recovery from wet biomass waste. In this study, the hydrothermal treatment of dewatered waste-activated sludge (DWAS) was evaluated at several temperatures (170–230 °C) and reaction times (5–60 min) in an acid-free medium or in media such as citric acid or HCl (0.1–0.5 mol/L). Compared with the DWAS, an increase in the fixed carbon content (>45 wt%) and heating value (18.9–22.9 MJ/kg) was observed in the hydrochar; however, their ash content remained high, which is the main drawback hindering their direct use as a biofuel. The addition of acids during hydrothermal treatment favored the solubilization of N and P in the process water, which required strict control of the reaction time to avoid the recrystallization of P in the hydrochar. Under optimum operating conditions (230 °C, 15 min, 0.5 mol/L HCl), 94 % of P (as of PO_4) and almost 100 % of N (14 % as NH_4-N) present in the feedstock were concentrated in the process water.

1. Introduction

Currently, more than 10 million tons of sewage sludge (on a dry basis) are generated in Europe each year (Bianchini et al., 2016). According to the latest data from the Organization for Economic Co-operation and Development (OECD, 2018), existing sewage management procedures cause serious problems, making it necessary to seek alternatives to landfilling or agricultural deposition. Different types of sewage sludge (primary, secondary (or activated), mixed, and tertiary) that are generated in wastewater treatment plants present dissimilar compositions in terms of the inorganic element content (Al, Na, Mg, and K, among others) and harmful components, such as organic pollutants, heavy metals, or pathogens (Mattenberger et al., 2008; Xu et al., 2015). Typically, sewage sludge requires stabilization and/or dewatering prior to its final disposal (Merzari et al., 2019).

In the last two decades, studies on the thermal treatment of sewage sludge, such as by gasification (Quan et al., 2022), pyrolysis (Ghodke et al., 2021), and combustion (Ahn et al., 2020), have been conducted to reduce the waste volume, obtain new products, or recover valuable materials. However, these technologies required large amounts of energy, and also required pre-drying of the feedstock and strict control of gas emissions

* Corresponding author.
E-mail address: andres.sarrion@uam.es (A. Sarrion).

http://dx.doi.org/10.1016/j.scitotenv.2022.156494
Received 22 March 2022; Received in revised form 31 May 2022; Accepted 1 June 2022
Available online 3 June 2022

(Bolan et al., 2021). Recently, hydrothermal carbonization (HTC) has emerged as a thermal process that allows the treatment and stabilization of wet sewage sludge at mild temperatures (180–250 °C) and low residence times (5–240 min) under an autogenous pressure. During HTC, the oxygen and hydrogen contents of the feedstock decrease through hydrolysis, condensation, aromatization, dehydration, and decarboxylation reactions (He et al., 2022; Ipiales et al., 2021). The critical temperature for an effective HTC process primarily depends on the composition of the feedstock, particularly the content of lignin (Cao et al., 2021). The main products of HTC are a carbonaceous solid known as hydrochar, which possesses fuel properties similar to those of lignite; process water (PW) with large amounts of inorganic salts and organic compounds; and a gaseous phase consisting mainly of CO_2, which is not very significant at low and intermediate carbonization temperatures (Kruse et al., 2013).

Hydrochar has environmental applications as a soil amendment (Bargmann et al., 2014; Khosravi et al., 2022) and as a nutrient source (Becker et al., 2019; Fei et al., 2019). The physical and energetic properties of hydrochar make it suitable for use as a solid fuel (Marin-Batista et al., 2020; Ipiales et al., 2022), enhancer of anaerobic digestion (Kumar et al., 2021), CO_2 capture agent (Goel et al., 2021; Wang et al., 2021a), energy storage material in fuel cells, supercapacitors, and batteries (Arenas Esteban et al., 2020; Zhou et al., 2021; Arauzo et al., 2022), and as a precursor for adsorbents (Diaz et al., 2019; Román et al., 2020) and activated carbons (Belete et al., 2021; Kumar et al., 2020). The use of hydrochar as a solid biofuel is acquiring focus because 50–85 % of its energy is contained in the feedstock (Román et al., 2012; Ipiales et al., 2021). Further, hydrochar exhibits good combustion properties, such as a high "higher heating value" (HHV), high energy density (Ischia and Fiori, 2020), and low ash, nitrogen, and sulfur contents, thus producing less NO_x and SO_x during combustion than the feedstock (Marin-Batista et al., 2020). In addition, hydrochar combustion results in the emission of lesser greenhouse gases (18 kg CO_2 eq/t of hydrochar) than the direct combustion of garden and park waste or sewage sludge (≈72 kg CO_2 eq/t) (Medina-Martos et al., 2020).

Process water is a byproduct with the potential to recover energy and valuable elements because it contains a high content of organic matter, nutrients, and minerals. The anaerobic digestion of different types of biomass-derived PW has been explored previously, with a significant amount of methane from PW reported to be derived from sewage sludge (Ahmed et al., 2021), food waste (Mannarino et al., 2022), and garden and park waste (Ipiales et al., 2022; Suarez et al., 2022).

Sewage sludge is a microbial-rich feedstock mainly composed of proteins, with high N (>90 g/kg) and P (>120 g/kg) contents (Wang et al., 2018; Yang et al., 2020). Nutrient recovery from sewage sludge is of interest because it can mitigate the demand for nutrients in the synthesis of fertilizers to meet the needs of the agri-food sector (Shaddel et al., 2019). HTC allows the recovery of nutrients from PW by optimizing the operating conditions (temperature and reaction time). The fate of N and P from the HTC of biomass waste has been addressed in the literature, with studies typically concluding that these components are mainly affected by the temperature. He et al. (2022) reported that the effective temperature for protein hydrolysis is 250 °C in an acid-free medium, which is accelerated under HTC conditions and an acidic pH. Malhotra and Garg (2020) studied the fate of N and P in sewage sludge. They observed that P was mainly retained in the hydrochar (up to 70 %), while N was solubilized up to 57 % in the PW at 200 °C for 3 h. In the case of digested sludge, the use of a lower temperature and reaction time (170 °C for 1 h) allowed the solubilization of up to 80 % of N in the PW, but 60 % of P was still retained in the hydrochar (Ekpo et al., 2015). Simultaneously, increasing the HTC temperature favored the solubilization of P from the digested sewage sludge. Aragón-Briceño et al. (2017) achieved a release of up to 87 % P and 65 % N in PW at 250 °C. A similar trend was observed by Idowu et al. (2017) using food waste, who obtained maximum solubilizations of 60 and 70 % for N and P, respectively, at 225 °C for 4 h. These results indicate that rigorous HTC conditions favor P release from sewage-derived wastes, whereas there is no clear trend for N; therefore, further analysis is required.

More recently, studies have focused on the role of pH in the solubilization of P. Most of these studies showed that HTC under acidic conditions promoted P release into PW (Ekpo et al., 2016; Dai et al., 2017; Qaramaleki et al., 2020; Sarrion et al., 2021), because most of the P was in the form of insoluble inorganic P linked to multivalent metal elements (Fe, Ca, Al, and Mg) present in the feedstock. A study on the acid-mediated HTC of animal manure showed that the addition of inorganic acids (HCl and H_2SO_4) allowed the release of more than 95 % P and 60 % N at a lower acid concentration than when using organic acids (citric acid and acetic acid) at temperatures below 200 °C (Ekpo et al., 2016; Dai et al., 2017; Qaramaleki et al., 2020). Food waste has also been treated using acid-mediated HTC to solubilize nutrients into the PW. More than 95 % of N and P were solubilized using 0.5 mol/L (M) HCl at 170 °C (Sarrion et al., 2021).

Once N and P are concentrated in the PW, they can be recovered through different physicochemical processes. P is commonly recovered as struvite (which also contains N as NH_4-N) or hydroxyapatite by chemical precipitation, by adjusting the P:Mg or P:Ca molar ratio in the aqueous solution to close to 1:1 under a basic pH (Marin-Batista et al., 2020; Zhang et al., 2020). The obtained solids can be directly employed in agriculture because they are beneficial for the soil (Zhang et al., 2020). From effluents with high ammonia concentrations (3–4 g/L), N is recovered as $(NH_4)_2SO_4$ through air ammonia stripping (He et al., 2015).

Several authors have studied the fate of nutrients at the final HTC reaction times of sewage sludge, animal manure, digestates, and food waste, and concluded that nutrient release into PW is negatively affected by the presence of inorganics. However, there is scarce information regarding the evolution of nutrient concentrations during HTC. Hence, the primary novelty of this work is the analysis of the evolution of nutrients and that of other elements (Al, Ca, Fe, and Mg) in PW with the reaction time at two temperatures (170 and 230 °C) under acid-free and acid-mediated HTC (0.1–0.5 M citric acid and HCl). Based on the obtained information, an in-depth study of the reactions governing the composition of the PW and hydrochar and the optimum reaction conditions to maximize the nutrient concentration in the PW is conducted. The hydrochar characterization results are expected to provide insights into the conditions required to obtain a suitable solid biofuel.

2. Materials and methods

2.1. Dewatered waste-activated sludge

Waste-activated sludge was obtained from a membrane bioreactor in a cosmetic factory (Madrid, Spain) and was dehydrated using a filter press. The raw dewatered waste activated sludge (DWAS) was stored in 2 kg portions at −20 °C. The moisture content of the defrosted portions of the DWAS was in the range of 87–92 wt%. Table 1 lists the characteristics of the main feedstock.

2.2. Hydrothermal carbonization

The HTC of the DWAS (1.5 kg) was performed in an electrically heated ZipperClave stirred pressure vessel (4 L). The effects of the process temperature (170–230 °C), acid reagent (citric acid, 99 %, Sigma Aldrich; HCl, 37 %, Sigma Aldrich), and concentration (0.1–0.5 M) during the HTC reaction were studied using response surface methodology based on a central composite rotatable design with a duplicate of the central point. Using Minitab 19 software, six acid-mediated HTC experiments (four factorial points and two replicates of the central point) and three acid-free HTC experiments were performed in duplicate.

Several PW samples (40 mL) were collected from the reactor at 5, 15, 30, and 60 min using a cooling system. The reaction was stopped after 60 min and the reactor was cooled by running tap water using a coil inside the reactor. The PW and hydrochar were separated through vacuum filtration using 250 μm filters. The wet hydrochar was dried at 105 °C for 24 h, ground, and sieved to a particle size of 100–200 μm. The PW was filtered

Table 1
Main characteristics of feedstock and hydrochars[a] (d.b).

Sample	T – [acid]	Proximate analysis (wt%)				Ultimate analysis (wt%)					HHV (MJ/kg)
		Solid yield	Fixed Carbon	Volatile matter	Ash content	C	H	N	S	O	
DWAS	–	–	12.7 (0.4)	73.7 (1.1)	13.6 (0.7)	43.0 (0.3)	5.9 (0.1)	6.4 (0.0)	0.3 (0.0)	30.8 (0.1)	18.5 (0.1)
HC	170 °C	48.5 (1.9)	8.4 (0.2)	75.2 (0.3)	16.4 (0.9)	46.3 (0.2)	6.2 (0.1)	6.6 (0.1)	0.5 (0.1)	24.0 (0.2)	20.6 (0.0)
	200 °C	40.1 (2.3)	14.2 (0.3)	66.1(0.9)	19.7 (1.7)	49.4 (0.5)	6.0 (0.2)	6.4 (0.1)	0.4 (0.0)	18.1 (0.0)	21.9 (0.1)
	230 °C	29.7 (1.7)	17.2 (0.5)	54.0 (0.4)	28.8 (0.3)	50.5 (0.1)	5.6 (0.1)	6.3 (0.0)	0.4 (0.0)	8.4 (0.1)	22.4 (0.0)
HC-citric acid	170 °C - 0.1 M	48.3 (3.4)	13.6 (1.1)	71.5 (0.1)	14.9 (1.0)	44.8 (0.8)	5.9 (0.0)	6.2 (0.1)	0.2 (0.0)	28.0 (0.1)	19.2 (0.2)
	170 °C - 0.5 M	56.2 (1.4)	12.7 (0.4)	72.9 (0.6)	14.4 (0.2)	46.8 (0.2)	5.4 (0.1)	4.9 (0.0)	0.2 (0.0)	28.3 (0.1)	19.5 (0.1)
	200 °C - 0.3 M	47.7 (0.9)	23.5 (1.6)	60.2 (0.7)	16.3 (0.3)	51.5 (0.6)	5.8 (0.2)	4.6 (0.2)	0.2 (0.1)	21.6 (0.2)	22.2 (0.0)
	230 °C - 0.1 M	44.7 (0.3)	23.1 (0.2)	52.3 (0.6)	24.6 (0.5)	45.2 (0.1)	5.7 (0.0)	6.7 (0.1)	0.2 (0.1)	17.6 (0.2)	20.0 (0.1)
	230 °C - 0.5 M	54.5 (2.7)	24.8 (0.1)	58.4 (0.4)	16.8 (0.7)	49.4 (0.1)	5.6 (0.1)	5.7 (0.1)	0.2 (0.1)	22.3 (0.0)	20.8 (0.1)
HC-HCl	170 °C - 0.1 M	51.1 (1.1)	10.7 (0.2)	67.9 (0.2)	21.4 (0.3)	45.8 (0.4)	5.7 (0.0)	6.4 (0.1)	0.3 (0.0)	20.4 (0.0)	19.9 (0.1)
	170 °C - 0.5 M	42.8 (2.3)	22.7 (0.3)	59.5 (1.2)	17.8 (1.6)	51.4 (0.3)	6.0 (0.1)	4.0 (0.0)	0.2 (0.0)	20.6 (0.2)	22.5 (0.1)
	200 °C - 0.3 M	47.3 (0.4)	18.8 (1.1)	61.9 (0.6)	19.3 (0.3)	50.5 (0.2)	5.8 (0.0)	5.0 (0.2)	0.2 (0.0)	19.2 (0.1)	21.9 (0.2)
	230 °C - 0.1 M	35.8 (2.4)	18.4 (1.2)	50.9 (0.4)	30.7 (1.3)	45.7 (0.1)	5.0 (0.0)	5.9 (0.0)	0.2 (0.0)	12.5 (0.1)	19.9 (0.2)
	230 °C - 0.5 M	31.9 (1.8)	26.1 (1.5)	48.5 (0.2)	25.4 (2.6)	46.8 (0.2)	4.8 (0.2)	3.7 (0.0)	0.1 (0.0)	19.2 (0.0)	19.5 (0.0)

[a] Data obtained after 60 min reaction time.

through 0.45 μm Scharlab syringe filters and stored at 4 °C. The mass yield of the hydrochar ($Y_{hydrochar}$) was calculated using Eq. (1) and defined as the ratio of the weight of the recovered hydrochar ($W_{hydrochar}$) to that of the DWAS feedstock (W_{DWAS}) on a dry basis.

$$Y_{hydrochar}\ (\%) = \left(W_{hydrochar}/W_{DWAS}\right)\cdot 100 \quad (1)$$

The yield of the PW (Y_{PW}) was calculated as the ratio of the total solids in the PW (W_{PW}) to that in the raw DWAS (W_{DWAS}) on a dry basis (Eq. (2)).

$$Y_{PW}\ (\%) = (W_{PW}/W_{DWAS})\cdot 100 \quad (2)$$

2.3. Analytical methods

The elemental composition (C, H, N, and S) of the PW and hydrochar samples was determined using a CHNS analyzer (LECO CHNS-932). ASTM methods (D3173–11, D3174–11, and D3175–11) were used to determine the moisture, ash, volatile matter, and fixed carbon contents (by difference) in the hydrochar. The oxygen content was calculated as the difference between the sum of the elemental contents and ash content. The HHV of the dry solid samples was determined using Eq. (3), which provides a relation between the HHV (MJ/kg) and C, H, N, S, O, and ash contents (in wt%) according to the work by Channiwala and Parikh (2002).

$$HHV\ (MJ/kg) = 0.349\cdot C + 1.178\cdot H + 0.100\cdot S - 0.103\cdot O - 0.015\cdot N - 0.021\cdot Ash \quad (3)$$

The hydrochar and PW were also analyzed using inductively coupled optical emission spectroscopy (Thermo Fisher Scientific IRIS INTREPID II XDL) to determine the concentration of the inorganic elements (Al, Ca, Fe, Mg, and P). The total Kjeldahl nitrogen in the PW was determined by digestion, distillation, and titration according to the standard method 4500-Norg-B published by the American Public Health Association (APHA, 2005). The NH_4-N content was evaluated by distillation and titration according to the standard method 4500-NH_3-B-C (APHA, 2005). The NO_2-N and NO_3-N contents were determined using a Dionex ICS-900 ion chromatograph with chemical suppression and fitted with a 4 × 250 mm Dionex IonPac AS22 column using 1 mL min^{-1} mobile phases of 1.4/4.5 mM $NaHCO_3$ and Na_2CO_3, respectively. Orthophosphate (PO_4-P) was determined photometrically using the Hach Lange LCK350 cuvette test. The results corresponding to P and N solubilization were also expressed as grams of P or N per kg of dry feedstock, by considering the volume of the PW in the mass balance.

3. Results and discussion

3.1. Characterization of the DWAS and HTC-treated hydrochar

Table 1 shows the proximate and ultimate analysis results of the DWAS and hydrochar obtained after a reaction time of 60 min. The DWAS contains 9 wt% solids, with N and P contents of 64 and 23.6 g/kg, respectively. Its main mineral elements are Al (1.6 wt%), Ca (1.7 wt%), and Mg (0.3 wt %). The HHV of DWAS is 18.5 MJ/kg, which is in the HHV range of biomass fuels (15–20 MJ/kg), primarily because of its high fixed carbon and lipid contents (Pradhan et al., 2018).

The hydrochar yields in the acid-free HTC experiments are above 40 % at temperatures between 170 and 200 °C and decrease to 29.7 % at 230 °C. In the citric acid-mediated HTC, the mass yield increases with the carbonization temperature because citric acid evolves during the hydrothermal reaction, producing other acids (e.g., acetic or formic acid) or decomposing into itaconic and citraconic acids, which affect the hydrolysis, dehydration, condensation, and polymerization reactions, thereby making the process autocatalytic and increasing the generation of secondary hydrochar when interacting with mineral compounds (Rodriguez Correa et al., 2017; He et al., 2022). The catalytic effect of some organic acids (formic acid, acetic acid, and glycolic acid) on the generation of hydrochar has been previously reported (Heidari et al., 2018; Wang et al., 2019; Hammerton and Ross, 2022). In contrast to citric acid, increasing the HCl concentration causes a significant decrease in the hydrochar yield because strong mineral acids increase the solubilization of mineral salts and increase the transfer of carbon to the PW (Szögi et al., 2015; Dai et al., 2017).

The use of more severe HTC conditions (acid-free and acid-mediated) resulted in hydrochar with more fixed carbon and less volatile matter due to the breakdown of oxygen-containing functional groups under hydrothermal conditions (Cao et al., 2013). Consequently, the elemental composition of the hydrochar was significantly different from that of the DWAS and depended on whether the HTC was acid-free or acid-mediated. Overall, hydrothermal treatment resulted in the formation of hydrochar with an increased C/O ratio and ash content, which was more evident in HCl-mediated hydrochar, thereby enhancing the removal of N and S, especially with increasing acid concentration.

The HHV of the hydrochar was higher than that of lignite (16–17 MJ/kg) (Engin et al., 2019) and comparable to those of different organic wastes such as anaerobic granular sludge (Yu et al., 2018), wheat straw (Reza et al., 2015) and animal manure (Dai et al., 2017). A positive trend in the HHV with increasing temperature was observed for hydrochar from acid-free HTC, which was attributed to a higher degree of carbonization of the solid. A similar trend was observed in citric acid-mediated HTC due to the increase in the C content of hydrochar associated with the increased solid yield; this is because citric acid promoted hydrolysis, thereby enhancing

repolymerization (He et al., 2022). For the hydrochar obtained by HCl-mediated HTC, the highest HHV was obtained from the sample processed at 170 °C with an acid concentration of 0.5 M because of the high solubilization of inorganic compounds to the PW, which caused a significant increase in the C content in the hydrochar. The fuel ratio (FC/VM) of the hydrochar was lower than 2.5, the optimum value required for their use as a solid biofuel in pulverized combustion systems (He et al., 2013), but increased with the temperature and acid concentration. A reduction in the volatile matter (<75 %), ash (<10 %), N (<3 %), and S (<0.2 %) contents, along with an HHV > 17 MJ/kg, are essential for using hydrochar as a solid biofuel in industrial applications, according to ISO/TS 17225–8 for thermally treated and densified biomass fuels. However, all the hydrochar obtained after a reaction time of 60 min contained >3 % N, and only hydrochar from 0.5 M HCl-mediated HTC approached this limit, enabling their use through blending with coal with a lower N content. Based on the hydrochar composition, the amount of N depended on the Mannic and Maillard reactions (which may result in the formation of N-containing heterocyclic compounds including quaternary-N and pyridine-N), although N repolymerization could be limited by shortening the reaction time (Villamil et al., 2020a).

3.2. Fate of P in the PW throughout hydrothermal treatment

Fig. 1 shows the evolution of P release into the PW during the hydrothermal reaction under different conditions. The P speciation analysis indicates that P is present in the PW only in the form of orthophosphate (PO_4-P). In acid-free HTC (Fig. 1a), the maximum P concentration in the PW (0.64 g/L) is attained at 5 min, regardless of the reaction temperature, which is equivalent to 5.8 g P/kg DWAS; this value remains constant over time at 230 °C. However, at lower temperatures, the P concentration decreases by up to 30 % after 60 min because of the lower likelihood of the precipitation of P with mineral compounds and the solubilization of PO_4-P from the decomposition of organic P (complex fractions including phospholipids, DNA, and phosphate monoesters) (Ekpo et al., 2015).

In citric acid-mediated HTC (Fig. 1b), the highest P concentrations in the PW are obtained at 15 min, regardless of the temperature and acid concentration. From this reaction time onwards, the P concentration decreases progressively until it reaches values similar to those obtained in the acid-free PW. The maximum P concentration is achieved at 170 °C using 0.5 M citric acid (10.4 g P/kg DWAS), although most of the P is still retained in the hydrochar. Thus, an increase in the temperature and a low acid concentration do not favor P leaching into the PW. Furthermore, the leaching effect of citric acid at 230 °C is not significant. This is because organic acids tend to decompose at elevated temperatures, generating CO_2, which in turn increases the pressure inside the reactor. This promotes dehydration and polymerization reactions between organic compounds and inorganics, including PO_4-P, which precipitates as a secondary hydrochar (He et al., 2022). Ekpo et al. (2016) observed a similar effect of the temperature with the addition of 0.1 M formic acid or 0.1 M acetic acid in the hydrothermal treatment of swine manure (16 g P/kg manure), and achieved releases of 3.0 and 3.2 g P/kg manure, respectively, into the PW at 170 °C.

In HCl-mediated HTC (Fig. 1c), the HCl concentration has a significant effect on P solubilization, while the temperature only has a minor impact. Under acidic conditions, the protein decomposition of DWAS microorganisms is accelerated, promoting the release of most of the organic P. Subsequently, the organic P is transformed into inorganic P under acid-catalyzed HTC conditions (Zhang et al., 2020). P release using 0.1–0.3 M HCl is not improved in acid-free HTC or citric acid-mediated HTC. Simultaneously, the addition of 0.5 M HCl results in a maximum P concentration (2.7 g/L) in the PW after 15 min at 230 °C, a value that is 90 % higher than those obtained with citric acid under the best operating conditions (1.4 g/L at 170 °C and 0.5 M citric acid after 15 min). In contrast, operating conditions of 30 min at 170 °C and the addition of 0.5 M HCl are necessary to reach the maximum P concentration (2.1 g/L) in the PW.

In all experiments, a significant decrease in the P concentration in the PW with the reaction time was observed after attaining the maximum concentration. This decrease in the available P can be attributed to the formation of insoluble P complexes such as $AlPO_4$, which could be retained within the hydrochar or precipitated as secondary hydrochar (Ovsyannikova et al., 2019; Qaramaleki et al., 2020).

In this study, the high Al concentration in the DWAS, arising from the use of Al salts during the coagulation step in the wastewater treatment, initially favored the reaction of Al^{3+} with PO_4^{3-}, whereas the reaction of PO_4^{3-} with Ca^{2+}, Mg^{2+}, and Fe^{2+} commenced when Al^{3+} was substantially consumed (Fig. 2). In acid-free HTC at 170 °C (Fig. 2a), a decrease in the P concentration occurred after a reaction time of 15 min; similar tendencies were observed for the Ca and Mg concentrations. This reduction may be associated with the precipitation of calcium and magnesium phosphates. The formation of calcium phosphate under hydrothermal conditions has been observed at pH levels above 4.8 and a Ca/P molar ratio between 2.3 and 2.5 (Mekmene et al., 2009). Magnesium phosphate can precipitate as struvite at a Mg/P molar ratio of 1–1.5 and pH close to 9 (Stratful et al., 2001), although a PW pH of 5.8 would allow the minimal precipitation of this compound. Thus, considering the obtained results, the decrease in the P, Ca, and Mg concentrations possibly allows the formation of Ca/P and Mg/P compounds with molar ratios in the ranges of 1.8–2.5 and 1.1–1.5, respectively. Fig. 2b indicates a lack of dissolved metals in the PW, suggesting that the temperature increase to 230 °C is crucial for retaining them within the hydrochar. As shown in Fig. 2c, e, and f, the formation of P complexes can be attributed mainly to Al because its concentration decreases at the same time as that of P. Fig. 2d shows that metals and P are not solubilized with citric acid at 230 °C and are mainly retained within the hydrochar. The increase in the concentration of the other metals compared to those in acid-free HTC indicates that they precipitate, especially as $AlPO_4$, under

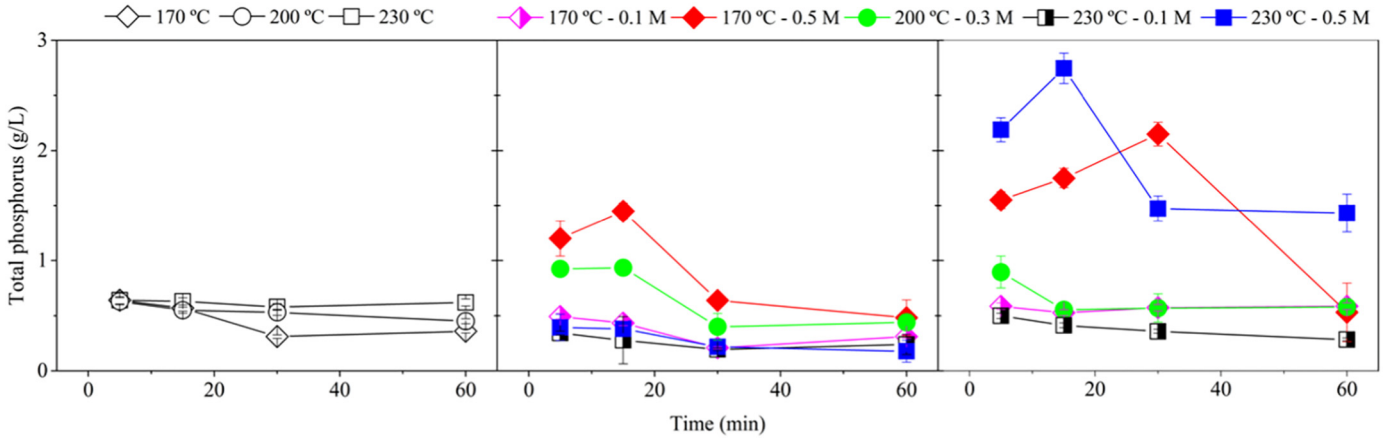

Fig. 1. Time course of phosphorous in process water for acid-free (a), citric acid-mediated (b) and HCl-mediated HTC (c).

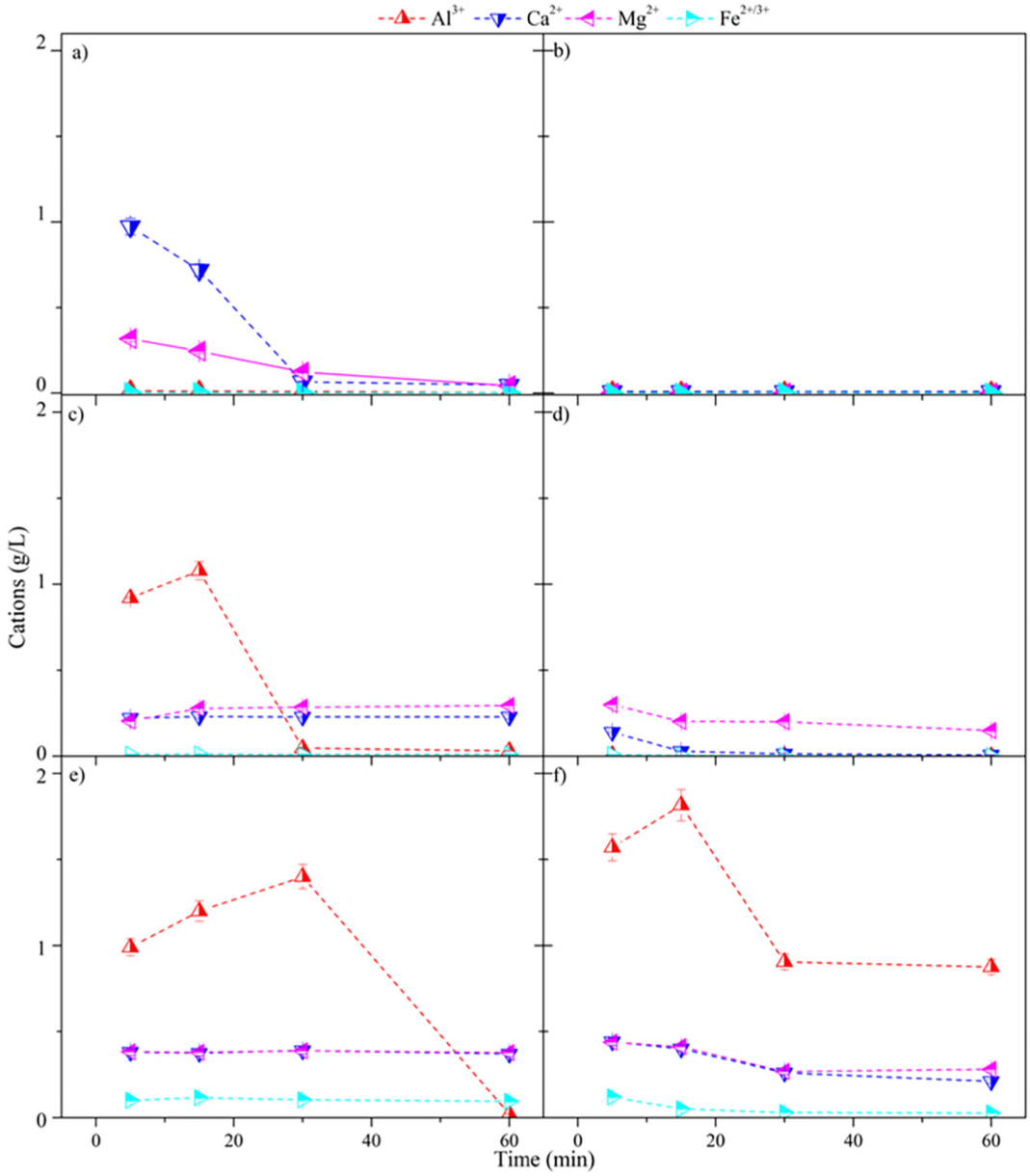

Fig. 2. Time course of the main cations in the process water for acid-free (a, b), 0.5 M citric acid-mediated (c, d) and 0.5 M HCl-mediated HTC (e, f) at 170 °C (left graphs) and 230 °C (right graphs).

these acidic conditions. This is mainly attributed to the effect of the pH on the phosphate species present in the reaction medium. At a pH below 4.8, phosphate anions exist primarily in their monobasic form ($H_2PO_4^-$), which facilitates the formation of acid phosphates with cations such as Al^{3+}, whose bonding is favored by the decreased number of OH^- anions (Palacios et al., 2013). However, the formation of phosphates with cations such as Ca^{2+} or Mg^{2+} is not favored at very acidic pH levels. This is because there is a decrease in the oversaturation of the medium due to the protonation of the dibasic phosphate species (HPO_4^{2-}), which predominantly occurs at a pH above 4.8, and to which it has more affinity (Mekmene et al., 2009). Additionally, $AlPO_4$ precipitates earlier at a higher temperature, which can also be related to the lower temperature favoring the formation of non-precipitable PO_4^{3-} phases that persist for a certain period of time (Roncal-Herrero et al., 2009). On the other hand, at a high temperature, Al—P complexes are rapidly formed.

Response surface analysis was performed to evaluate the operating conditions to assess the solubilization of P (as PO_4-P) in the PW (Table 2). Based on previous results, a reaction time of 15 min was selected as optimal, and the temperature (°C) and acid concentration (M) were analyzed as input factors in citric acid-mediated (Eq. (4)) and HCl-mediated HTC (Eq. (5)):

The predictions of the P concentration in the PW by Eqs. (4) and (5) agreed with the experimental results ($p < 0.05$, $R^2 > 99.9$ %). The three-dimensional response surfaces of normalized P release in citric acid-mediated and HCl-mediated HTC are shown in Fig. 3a and d, respectively. The normalized P concentration in the PW at 15 min for citric acid-mediated HTC reaches a maximum of 47 % of the total P concentration in the DWAS at 170 °C using 0.5 M citric acid. In HCl-mediated HTC, the normalized P concentration in the PW is almost equivalent to the total P concentration in the DWAS (94 %) at 230 °C using 0.5 M HCl. HCl solubilizes more P in the PW than citric acid, which mainly catalyzes hydrochar formation, allowing P to be retained in the solid. These results are consistent with those obtained by Dai et al. (2017) for the HCl-mediated HTC (2 wt%) of manure at 190 °C, where 95 % P was leached into the PW as PO_4-P. Furthermore, Sarrion et al. (2021) noted that the HCl-mediated HTC of food waste at 170 °C allowed the recovery of 98 % of the initial P in the PW after 60

Table 2
Descripting equations of normalized P, N and NH_4-N solubilization as a function of temperature (T, °C) and acid concentration (C, M) at 15 min reaction time.

Citric acid-mediated HTC	R^2	Eq.	HCl-mediated HTC	R^2	Eq.
$P/Po = 0.2508 - 0.001167 \cdot T + 1.108 \cdot C - 0.00167 \cdot T \cdot C$	99.99	(4)	$P/Po = 0.4918 - 0.003167 \cdot T - 2.967 \cdot C + 0.02333 \cdot T \cdot C$	99.98	(5)
$N/No = 0.00167 \cdot T - 0.133 \cdot C + 0.00167 \cdot T \cdot C + 0.18895$	99.96	(6)	$N/No = 0.43465 - 0.000458 \cdot T - 0.829 \cdot C + 0.009583 \cdot T \cdot C$	99.97	(7)
$NH_4 - N/No = 0.000017 \cdot T + 0.059 \cdot C + 0.000467 \cdot T \cdot C + 0.01545$	99.98	(8)	$NH_4 - N/No = 0.089 \cdot T + 39.7 \cdot C - 0.129 \cdot T \cdot C - 12.7665$	99.94	(9)

min. These results highlight the potential of this process as an alternative to P recovery from biomass waste via non-acidified HTC, particularly for food waste (70 % P recovery at 225 °C) (Idowu et al., 2017) or poultry litter (45 % P recovery at 230 °C) (Ismail et al., 2019).

3.3. Fate of N in the PW throughout hydrothermal treatment

A similar analysis was performed for the N in the PW. Hydrothermal conditions allowed the hydrolysis of proteins, amino acids, and multi-peptides present in the DWAS, resulting in the solubilization of different N compounds to the PW (Jiang et al., 2010). In acid-free HTC (Fig. 4a), the N release is positively affected by the temperature, as observed in the first 5–30 min of the reaction, where increased N solubilization is observed with an increase in temperature up to 230 °C. However, a similar value of 3.9 g N/L (31.2 g N/kg DWAS) is observed after 30 min regardless of the HTC temperature.

As shown in Fig. 4b, for a given temperature, citric acid does not affect N solubilization into the PW during the reaction. However, the temperature has a significant effect on N solubilization. The acid concentration is also a contributing factor (but to a lesser degree) to the increase in the concentration of solubilized N by 45 % in the experiment at 230 °C using 0.5 M citric acid (42.4 g N/kg DWAS) with respect to that performed at 170 °C

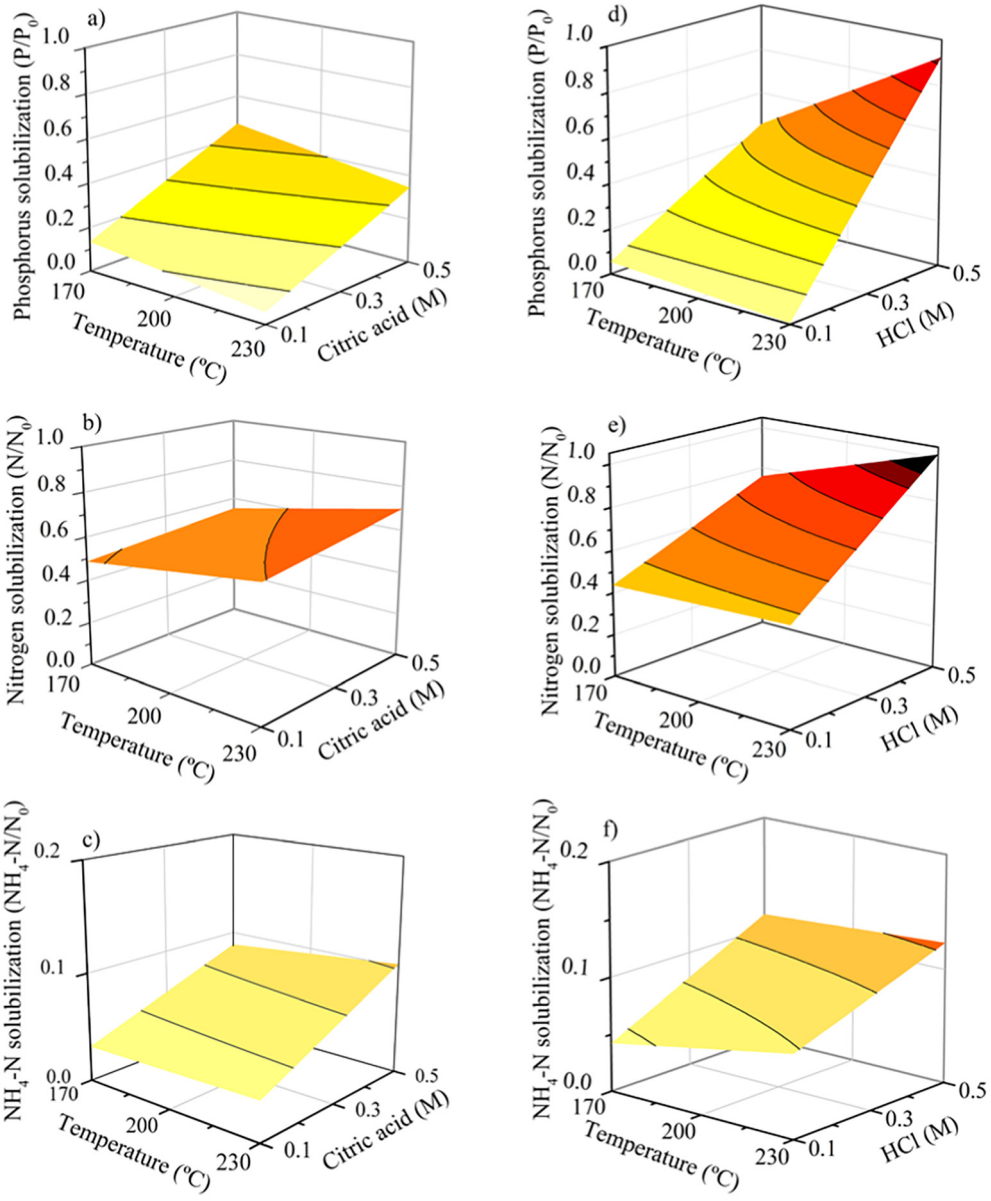

Fig. 3. Response surface of normalized P (a, d), N (b, e), and NH_4-N (c, f) concentration in the process water for citric acid-mediated (left graphs) and HCl-mediated HTC (right graphs) at 15 min reaction time.

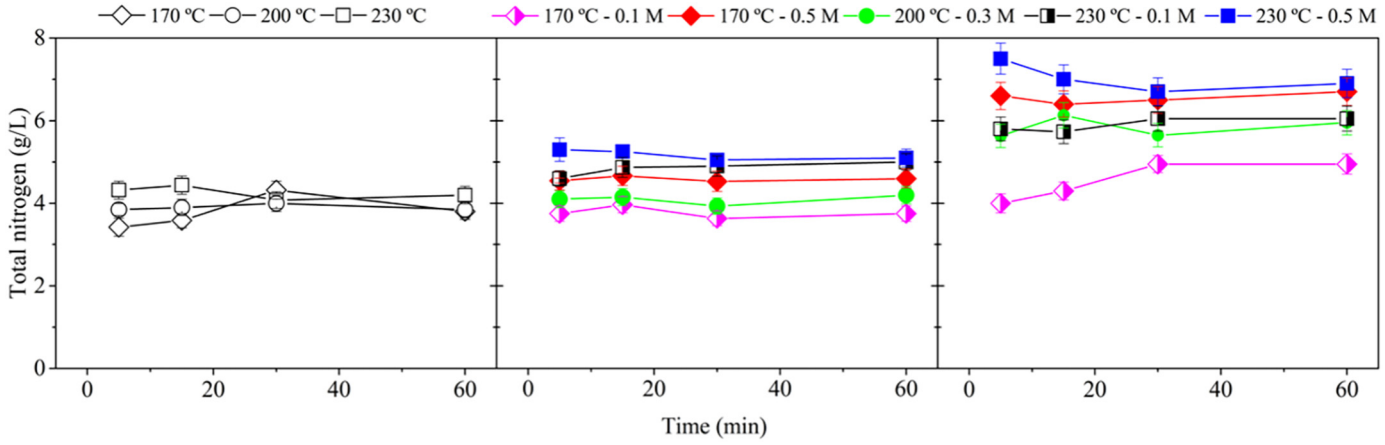

Fig. 4. Time course of nitrogen in process water for acid-free (a), citric acid-mediated (b) and HCl-mediated HTC (c).

using 0.1 M citric acid. The amount of N obtained in the PW at temperatures below 200 °C and a citric acid concentration lower than 0.3 M is similar to that obtained during acid-free HTC, rendering more severe conditions essential for N release from hydrochar (Sengupta et al., 2015; Wang et al., 2021b).

Fig. 4c shows the N leaching amount in the PW during HCl-mediated HTC, which increases with the temperature and HCl concentration in the following order: 230 °C–0.5 M > 170 °C–0.5 M > 230 °C–0.1 M ≥ 200 °C–0.3 M > 170 °C–0.1 M). This indicates that the acid concentration has a stronger effect on N solubilization than the temperature. The maximum N concentration in the PW is 7.5 g/L (63 g N/kg DWAS), recorded in the first 5 min of the reaction, and decreases slightly until 30 min because of the possible retention of N compounds within the hydrochar, remaining constant thereafter. This N concentration was always higher than that obtained in acid-free and citric-acid-mediated HTC.

To establish a compromise between the maximum P and N concentrations in the PW, a reaction time of 15 min was selected to perform the three-dimensional N recovery response surface analysis using citric acid and HCl as acid reagents. Analysis of the N species present in the PW (Fig. 5) showed that the N solubilized using citric acid was mostly in the form of N-bearing organic compounds (>85 %) and NH_4-N (2–10 %). When using HCl, especially at concentrations higher than 0.3 M, N was solubilized mainly as organic N (40–70 %), NO_3-N (10–40 %), and NH_4–N (10–20 %).

Fig. 3b, c, e, and f show the response surface results of N recovery in the PW as total N and NH_4-N after a reaction time of 15 min, highlighting its relevance as a fertilizer constituent. Table 2 lists the equations for the solubilization of N (Eqs. (6) and (7)) and NH_4-N (Eqs. (8) and (9)) after this period of citric acid-mediated and HCl-mediated HTC, respectively, as a function of the temperature (°C) and acid concentration (M). The obtained fit is statistically significant ($p < 0.05$, $R^2 > 99.9$ %).

For both acids, the highest N solubilization in the PW is observed at the highest studied temperature (230 °C) and acid concentration (0.5 M). Approximately 69 % N (44.2 g N/kg DWAS) is solubilized during citric acid-mediated HTC and practically all the N (63.4 g N/kg DWAS) is solubilized during HCl-mediated HTC. However, only 10 and 13 % of N are leached as NH_4-N during citric acid- and HCl-mediated HTC, respectively. This is because N is mainly released as organic N, which can be hydrothermally decomposed to NH_4-N at higher temperatures and reaction times (He et al., 2015). The NH_4-N concentrations slightly increase during citric acid-mediated and HCl-mediated HTC, reaching maximum values of 0.9 g/L (7.7 g NH_4-N/kg DWAS) and 1.4 g/L (12.4 g NH_4-N/kg DWAS), respectively, after 60 min. These concentrations are 16 and 20 % higher than those observed at 15 min and are equivalent to 12 and 20 % of the total N contained in the feedstock, respectively. This result indicates that the transformation of organic N to NH_4-N occurs with increasing reaction time. Previous studies have shown that the N species found in PW are related to the characteristics of the starting biomass waste. Similar NH_4-N concentrations in the PW (26 % of the N contained in the starting biomass) were determined in the effluent obtained from hydrothermal septic water treatment at 220 °C for 120 min (McGaughy and Reza, 2018), whereas

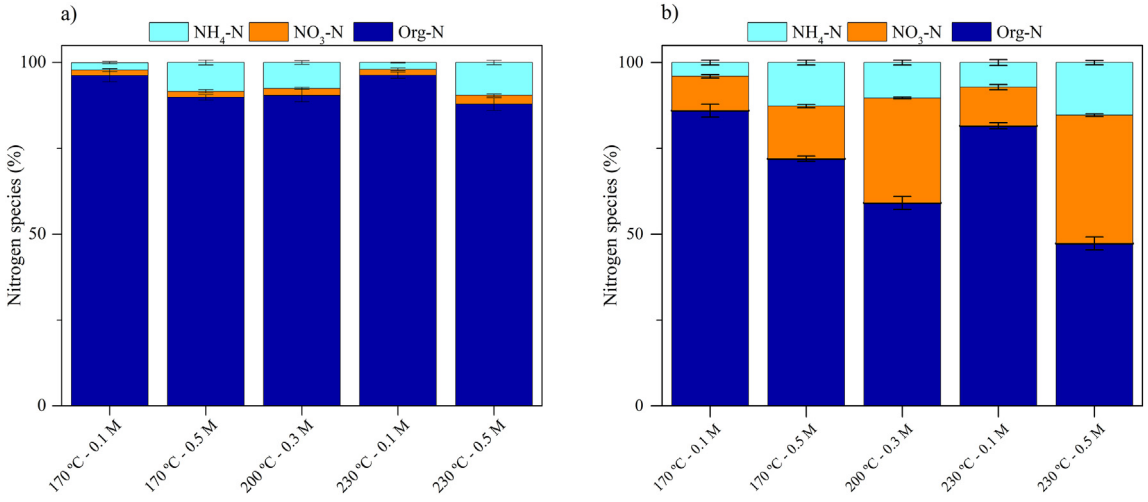

Fig. 5. Distribution of nitrogenous species in process water at 15 min for citric acid-mediated (a) and HCl-mediated (b) HTC.

the highest ammonium concentration (48 % of total N) was obtained from cattle manure treated at 190 °C for 12 h (Dai et al., 2017).

3.4. Economic outlook of HCl-mediated HTC technology

The remarkable impact of mineral acids on the fate of P and N throughout the HTC of DWAS is notable, but would increase the cost of the process in future scale-ups. Under the optimized conditions, a low HCl concentration is required to significantly solubilize the nutrients in the PW, offering the possibility of recovering them in the form of value-added compounds such as struvite or hydroxyapatite (Becker et al., 2019; Marin-Batista et al., 2020). These products are economically viable and profitable in commercial agricultural applications. A preliminary economic study of the HCl-mediated HTC process was performed based on the energy inputs (reaction, slurry separation, and hydrochar drying) and cost of the reagents. The HTC reactor presented considerable versatility (it allowed a batch or continuous configuration) and performance during the reaction, with no significant variations in the characteristics of the resulting products. The energy input required to heat the reactor (1.5 m^3), which was operating continuously, to attain the optimum operating conditions for optimum P and N solubilization (230 °C and 15 min), was determined. Considering the energy integration of the streams for heat recovery, the energy requirements of the process could be optimized by preheating the inlet stream to 100 °C using the heat energy from the reactor outlet stream. The energy inputs (kJ/kg) were calculated using Eq. (10).

$$E_{preheat\ -\ HTC,in} = \lfloor m_L \cdot C_L + m_s \cdot C_{DWAS} \rfloor \cdot (T_{HTC} - T_{373K}) \quad (10)$$

where m_L is the liquid content of the DWAS; C_L is the specific heat of the liquid fraction of the DWAS, which was assumed to be water (4.18 kJ/kg·K); m_S is the dry solid content of the DWAS; and C_{DWAS} is the specific heat of the DWAS (2.83 kJ/kg·K), calculated using the Aspen Plus simulator. Considering the cost of the required HCl amount and energy inputs (85.9 €/MWh (Eurostat, 2022)), the cost of the HTC process was estimated to be approximately 12.5 € per ton of DWAS. Hence, this process is inexpensive compared to that reported by Vardanyan et al. (2018), who carried out a sequential extraction with the addition of heterotrophic acidophilic iron-reducing bacteria to solubilize P from DWAS (114 €/ton raw DWAS). Moreover, this technique appears to be more economically effective than that of Zhang et al. (2020), who used HCl and H_2O_2 to promote P release from swine manure digestate under hydrothermal conditions for struvite precipitation (16.7 €/ton raw digestate). For P and N recovery from struvite, the cost of the required reagents can be calculated according to previous studies (Munir et al., 2017; Becker et al., 2019; Zhang et al., 2020). For struvite crystallization, it is necessary to adjust both, the Mg:P molar ratio in the PW (containing 2.75 g P/L and 0.4 g Mg/L) and the pH. Therefore, considering $MgCl_2$ and NaOH, the cost of total reagent addition was calculated to be approximately 1.2 €/ton DWAS (Munir et al., 2017; Becker et al., 2019). The cost of chemicals was 1.3 €/ton of wastewater for struvite precipitation (Huang et al., 2015) and lower than the 1.9 € per ton cost of swine manure digestate (Zhang et al., 2020). Nutrient-depleted PW can still contain a large amount of dissolved organic compounds. Hence, it would be interesting to explore new methods such as aqueous phase reforming or anaerobic digestion (Oliveira et al., 2022; Villamil et al., 2020b) to obtain a biogas stream that could improve the energy recovery of DWAS and reduce the energy demand of the process.

The presented HCl-mediated HTC process is the first step in obtaining high-quality struvite to improve the characteristics of hydrochar. Future work should focus on (i) establishing a relationship between the DWAS characteristics and the selection of the best conditions for nutrient recovery from PW; (ii) improving the quality of the PW and struvite; (iii) evaluating the characteristics of hydrochar as a biofuel working at low reaction times; (iv) overall energy balance, techno-economic, and life cycle assessments of an integrated system for acid-mediated HTC; and (v) scaling up DWAS treatment by HTC for nutrient recovery and biofuel production.

4. Conclusions

The acid-mediated hydrothermal treatment of sewage sludge favored the leaching of P (PO_4-P) and N (as organic nitrogen and NH_4-N) into the PW. Nutrient solubilization was improved by increasing the acid concentration and, to a lesser extent, by increasing the temperature, with the optimum conditions being 230 °C for 15 min and the use of 0.5 M HCl. The fate of P in the PW was determined by the reaction time because of the complexation and precipitation of the phosphate with the dissolved metal cations. In addition to recovering nutrients, the HCl-mediated HTC of sewage sludge generated hydrochar with attractive characteristics for use as a blended industrial biofuel.

CRediT authorship contribution statement

Andres Sarrion: Investigation, Formal analysis, Writing – original draft. **Angeles de la Rubia:** Funding acquisition, Writing – review & editing, Supervision. **Charles Coronella:** Writing – review & editing, Supervision. **Angel F. Mohedano:** Conceptualization, Funding acquisition, Methodology, Resources, Writing – review & editing, Supervision, Project administration. **Elena Diaz:** Conceptualization, Formal analysis, Funding acquisition, Methodology, Resources, Writing – review & editing, Supervision.

Declaration of competing interest

The authors declare that they have no known competing financial interests or personal relationships that could have appeared to influence the work reported in this paper.

Acknowledgments

The authors greatly appreciate funding from the Spanish MICINN (Project PID2019-108445RB-I00; PDC2021-120755-I00), Madrid Regional Government (Project S2018/EMT-4344), and US National Science Foundation (NSF #CBET-1856009). A. Sarrion wishes to thank the Spanish MICINN and ESF for a research grant (BES-2017-081515).

References

Ahmed, M., Andreottola, G., Elagroudy, S., Negm, M.S., Fiori, L., 2021. Coupling hydrothermal carbonization and anaerobic digestion for sewage digestate management: influence of hydrothermal treatment time on dewaterability and bio-methane production. J. Environ. Manag. 281, 111910. https://doi.org/10.1016/J.JENVMAN.2020.111910.

Ahn, H., Kim, D., Lee, Y., 2020. Combustion characteristics of sewage sludge solid fuels produced by drying and hydrothermal carbonization in a fluidized bed. Renew. Energy 147, 957–968. https://doi.org/10.1016/j.renene.2019.09.057.

APHA, 2005. Standard Methods for Examination of Water And Wastewater. 21st ed. American Public Health Association/American Water Works Association/Water Environment Federation, Washington DC.

Aragón-Briceño, C., Ross, A.B., Camargo-Valero, M.A., 2017. Evaluation and comparison of product yields and bio-methane potential in sewage digestate following hydrothermal treatment. Appl. Energy 208, 1357–1369. https://doi.org/10.1016/j.apenergy.2017.09.019.

Arauzo, P.J., Maziarka, P.A., Schoder, K.A., Pfersich, J., Ronsse, F., Kruse, A., 2022. Influence of sequential HTC pre-treatment and pyrolysis on wet food-industry wastes: optimisation toward nitrogen-rich hierarchical carbonaceous materials intended for use in energy storage solutions. Sci. Total Environ. 816, 151648. https://doi.org/10.1016/J.SCITOTENV.2021.151648.

Arenas Esteban, D., Guerrero Martínez, A., Carretero González, J., Birss, V.I., Otero-Díaz, L.C., Ávila Brande, D., 2020. Tunable supercapacitor materials derived from hydrochar/gold nanograpes. ACS Appl. Energy Mater. 3, 9348–9359. https://doi.org/10.1021/ACSAEM.0C01711/SUPPL_FILE/AE0C01711_SI_002.MP4.

Bargmann, I., Rillig, M.C., Kruse, A., Greef, J.-M., Kücke, M., 2014. Effects of hydrochar application on the dynamics of soluble nitrogen in soils and on plant availability. J. Plant Nutr. Soil Sci. 177, 48–58. https://doi.org/10.1002/jpln.201300069.

Becker, G.C., Wüst, D., Köhler, H., Lautenbach, A., Kruse, A., 2019. Novel approach of phosphate-reclamation as struvite from sewage sludge by utilising hydrothermal carbonization. J. Environ. Manag. 238, 119–125. https://doi.org/10.1016/j.jenvman.2019.02.121.

Belete, Y.Z., Ziemann, E., Gross, A., Bernstein, R., 2021. Facile activation of sludge-based hydrochar by Fenton oxidation for ammonium adsorption in aqueous media. Chemosphere 273, 128526. https://doi.org/10.1016/J.CHEMOSPHERE.2020.128526.

Bianchini, A., Bonfiglioli, L., Pellegrini, M., Saccani, C., 2016. Sewage sludge management in Europe: a critical analysis of data quality. Int. J. Environ. Waste Manag. 18, 226–238. https://doi.org/10.1504/IJEWM.2016.080795.

Bolan, N., Hoang, S.A., Beiyuan, J., Gupta, S., Hou, D., Karakoti, A., Joseph, S., Jung, S., Kim, K.H., Kirkham, M.B., Kua, H.W., Kumar, M., Kwon, E.E., Ok, Y.S., Perera, V., Rinklebe, J., Shaheen, S.M., Sarkar, B., Sarmah, A.K., Singh, B.P., Singh, G., Tsang, D.C.W., Vikrant, K., Vithanage, M., Vinu, A., Wang, H., Wijesekara, H., Yan, Y., Younis, S.A., Van Zwieten, L., 2021. Multifunctional applications of biochar beyond carbon storage. 67, pp. 150–200. https://doi.org/10.1080/09506608.2021.1922047.

Cao, X., Ro, K.S., Libra, J.A., Kammann, C.I., Lima, I., Berge, N., Li, A., Li, Y., Chen, N., Yang, J., Deng, B., Mao, J., 2013. Effects of biomass types and carbonization conditions on the chemical characteristics of hydrochars. J. Agric. Food Chem. 61, 9401–9411. https://doi.org/10.1021/jf402345k.

Cao, Y., He, M., Dutta, S., Luo, G., Zhang, S., Tsang, D.C.W., 2021. Hydrothermal carbonization and liquefaction for sustainable production of hydrochar and aromatics. Renew. Sustain. Energy Rev. 152. https://doi.org/10.1016/J.RSER.2021.111722.

Channiwala, S.A., Parikh, P.P., 2002. A unified correlation for estimating HHV of solid, liquid and gaseous fuels. Fuel 81, 1051–1063. https://doi.org/10.1016/S0016-2361(01)00131-4.

Dai, L., Yang, B., Li, H., Tan, F., Zhu, N., Zhu, Q., He, M., Ran, Y., Hu, G., 2017. A synergistic combination of nutrient reclamation from manure and resultant hydrochar upgradation by acid-supported hydrothermal carbonization. Bioresour. Technol. 243, 860–866. https://doi.org/10.1016/j.biortech.2017.07.016.

Diaz, E., Manzano, F.J., Villamil, J., Rodriguez, J.J., Mohedano, A.F., 2019. Low-cost activated grape seed-derived hydrochar through hydrothermal carbonization and chemical activation for sulfamethoxazole adsorption. Appl. Sci. 9, 5127. https://doi.org/10.3390/app9235127.

Ekpo, U., Ross, A.B., Camargo-Valero, M.A., Williams, P.T., 2015. A comparison of product yields and inorganic content in process streams following thermal hydrolysis and hydrothermal processing of microalgae, manure and digestate. Bioresour. Technol. 200, 951–960. https://doi.org/10.1016/j.biortech.2015.11.018.

Ekpo, U., Ross, A.B., Camargo-Valero, M.A., Fletcher, L.A., 2016. Influence of pH on hydrothermal treatment of swine manure: impact on extraction of nitrogen and phosphorus in process water. Bioresour. Technol. 214, 637–644. https://doi.org/10.1016/J.BIORTECH.2016.05.012.

Engin, B., Atakül, H., Ünlü, A., Olgun, Z., 2019. CFB combustion of low-grade lignites: operating stability and emissions. J. Energy Inst. 92, 542–553. https://doi.org/10.1016/j.joei.2018.04.004.

Eurostat, 2022. Electr. prices non-household Consum. - S1, 2022. DOI: https://ec.europa.eu/eurostat/databrowser/view/ten00117/default/table?lang=en (accessed 5.11.22).

Fei, Y.heng, Zhao, D., Liu, Y., Zhang, W., Tang, Y.yuan, Huang, X., Wu, Q., Wang, Y.xing, Xiao, T., Liu, C., 2019. Feasibility of sewage sludge derived hydrochars for agricultural application: Nutrients (N, P, K) and potentially toxic elements (Zn, Cu, Pb, Ni, Cd). Chemosphere 236, 124841. https://doi.org/10.1016/J.CHEMOSPHERE.2019.124841.

Ghodke, P.K., Sharma, A.K., Pandey, J.K., Chen, W.H., Patel, A., Ashokkumar, V., 2021. Pyrolysis of sewage sludge for sustainable biofuels and value-added biochar production. J. Environ. Manag. 298, 113450. https://doi.org/10.1016/J.JENVMAN.2021.113450.

Goel, C., Mohan, S., Dinesha, P., 2021. CO2 capture by adsorption on biomass-derived activated char: a review. Sci. Total Environ. 798, 149296. https://doi.org/10.1016/J.SCITOTENV.2021.149296.

Hammerton, J.M., Ross, A.B., 2022. Inorganic Salt Catalysed Hydrothermal Carbonisation (HTC) of Cellulose.

He, C., Giannis, A., Wang, J.Y., 2013. Conversion of sewage sludge to clean solid fuel using hydrothermal carbonization: hydrochar fuel characteristics and combustion behavior. Appl. Energy 111, 257–266. https://doi.org/10.1016/j.apenergy.2013.04.084.

He, C., Wang, K., Yang, Y., Amaniampong, P.N., Wang, J.Y., 2015. Effective nitrogen removal and recovery from dewatered sewage sludge using a novel integrated system of accelerated hydrothermal deamination and air stripping. Environ. Sci. Technol. 49, 6872–6880. https://doi.org/10.1021/acs.est.5b00652.

He, M., Zhu, X., Dutta, S., Khanal, S.K., Lee, K.T., Masek, O., Tsang, D.C.W., 2022. Catalytic co-hydrothermal carbonization of food waste digestate and yard waste for energy application and nutrient recovery. Bioresour. Technol. 344. https://doi.org/10.1016/J.BIORTECH.2021.126395.

Heidari, M., Salaudeen, S., Dutta, A., Acharya, B., 2018. Effects of process water recycling and particle sizes on hydrothermal carbonization of biomass. https://doi.org/10.1021/acs.energyfuels.8b02684.

Huang, H., Huang, L., Zhang, Q., Jiang, Y., Ding, L., 2015. Chlorination decomposition of struvite and recycling of its product for the removal of ammonium-nitrogen from landfill leachate. Chemosphere 136, 289–296. https://doi.org/10.1016/J.CHEMOSPHERE.2014.10.078.

Idowu, I., Li, L., Flora, J.R.V., Pellechia, P.J., Darko, S.A., Ro, K.S., Berge, N.D., 2017. Hydrothermal carbonization of food waste for nutrient recovery and reuse. Waste Manag. 105, 566–574. https://doi.org/10.1016/j.wasman.2017.08.051.

Ipiales, R.P., de la Rubia, M.A., Diaz, E., Mohedano, A.F., Rodriguez, J.J., 2021. Integration of hydrothermal carbonization and anaerobic digestion for energy recovery of biomass waste: an overview. Energy Fuel 35, 17032–17050. https://doi.org/10.1021/ACS.ENERGYFUELS.1C01681.

Ipiales, R.P., Mohedano, A.F., Diaz, E., de la Rubia, M.A., 2022. Energy recovery from garden and park waste by hydrothermal carbonisation and anaerobic digestion. Waste Manag. 140, 100–109. https://doi.org/10.1016/J.WASMAN.2022.01.003.

Ischia, G., Fiori, L., 2020. Hydrothermal carbonization of organic waste and biomass: a review on process, reactor, and plant modeling. Waste Biomass Valorization 126 (12), 2797–2824. https://doi.org/10.1007/S12649-020-01255-3.

Ismail, H.Y., Shirazian, S., Skoretska, I., Mynko, O., Ghanim, B., Leahy, J.J., Walker, G.M., Kwapinski, W., 2019. ANN-kriging hybrid model for predicting carbon and inorganic phosphorus recovery in hydrothermal carbonization. Waste Manag. 85, 242–252. https://doi.org/10.1016/j.wasman.2018.12.044.

Jiang, Z., Meng, D., Mu, H., Yoshikawa, K., 2010. Study on the hydrothermal drying technology of sewage sludge. Sci. China Technol. Sci. 53, 160–163. https://doi.org/10.1007/s11431-009-0423-7.

Khosravi, A., Zheng, H., Liu, Q., Hashemi, M., Tang, Y., Xing, B., 2022. Production and characterization of hydrochars and their application in soil improvement and environmental remediation. Chem. Eng. J. 430, 133142. https://doi.org/10.1016/J.CEJ.2021.133142.

Kruse, A., Funke, A., Titirici, M.M., 2013. Hydrothermal conversion of biomass to fuels and energetic materials. Curr. Opin. Chem. Biol. 17, 515–521. https://doi.org/10.1016/j.cbpa.2013.05.004.

Kumar, M., Xiong, X., Sun, Y., Yu, I.K.M., Tsang, D.C.W., Hou, D., Gupta, J., Bhaskar, T., Pandey, A., 2020. Critical review on biochar-supported catalysts for pollutant degradation and sustainable biorefinery. Adv. Sustain. Syst. 4, 1900149. https://doi.org/10.1002/ADSU.201900149.

Kumar, M., Dutta, S., You, S., Luo, G., Zhang, S., Show, P.L., Sawarkar, A.D., Singh, L., Tsang, D.C.W., 2021. A critical review on biochar for enhancing biogas production from anaerobic digestion of food waste and sludge. J. Clean. Prod. 305, 127143. https://doi.org/10.1016/J.JCLEPRO.2021.127143.

Malhotra, M., Garg, A., 2020. Hydrothermal carbonization of centrifuged sewage sludge: determination of resource recovery from liquid fraction and thermal behaviour of hydrochar. Waste Manag. 117, 114–123. https://doi.org/10.1016/J.WASMAN.2020.07.026.

Mannarino, G., Sarrion, A., Diaz, E., Gori, R., De la Rubia, M.A., Mohedano, A.F., 2022. Improved energy recovery from food waste through hydrothermal carbonization and anaerobic digestion. Waste Manag. 142, 9–18. https://doi.org/10.1016/J.WASMAN.2022.02.003.

Marin-Batista, J.D., Mohedano, A.F., Rodríguez, J.J., de la Rubia, M.A., 2020. Energy and phosphorous recovery through hydrothermal carbonization of digested sewage sludge. Waste Manag. 105, 566–574. https://doi.org/10.1016/j.wasman.2020.03.004.

Mattenberger, H., Fraissler, G., Brunner, T., Herk, P., Hermann, L., Obernberger, I., 2008. Sewage sludge ash to phosphorus fertiliser: variables influencing heavy metal removal during thermochemical treatment. Waste Manag. 28, 2709–2722. https://doi.org/10.1016/j.wasman.2008.01.005.

McGaughy, K., Reza, M.T., 2018. Recovery of macro and micro-nutrients by hydrothermal carbonization of septage. J. Agric. Food Chem. 66, 1854–1862. https://doi.org/10.1021/acs.jafc.7b05667.

Medina-Martos, E., Istrate, I.R., Villamil, J.A., Gálvez-Martos, J.L., Dufour, J., Mohedano, Á.F., 2020. Techno-economic and life cycle assessment of an integrated hydrothermal carbonization system for sewage sludge. J. Clean. Prod. 277, 122930. https://doi.org/10.1016/J.JCLEPRO.2020.122930.

Mekmene, O., Quillard, S., Rouillon, T., Bouler, J.M., Piot, M., Gaucheron, F., 2009. Effects of pH and Ca/P molar ratio on the quantity and crystalline structure of calcium phosphates obtained from aqueous solutions. Dairy Sci. Technol. 89, 301–316. https://doi.org/10.1051/dst/2009019.

Merzari, F., Langone, M., Andreottola, G., Fiori, L., 2019. Methane production from process water of sewage sludge hydrothermal carbonization. A review. Valorising sludge through hydrothermal carbonization. Crit. Rev. Environ. Sci. Technol. 49, 947–988. https://doi.org/10.1080/10643389.2018.1561104.

Munir, M.T., Li, B., Boiarkina, I., Baroutian, S., Yu, W., Young, B.R., 2017. Phosphate recovery from hydrothermally treated sewage sludge using struvite precipitation. Bioresour. Technol. 239, 171–179. https://doi.org/10.1016/j.biortech.2017.04.129.

OECD, 2018. Information environment database sewage sludge production and disposal. [WWW Document]. URL http://www.oecd.org/.

Oliveira, A.S., Sarrión, A., Baeza, J.A., Diaz, E., Calvo, L., Mohedano, A.F., Gilarranz, M.A., 2022. Integration of hydrothermal carbonization and aqueous phase reforming for energy recovery from sewage sludge. Chem. Eng. J. 442, 136301. https://doi.org/10.1016/J.CEJ.2022.136301.

Ovsyannikova, E., Arauzo, P.J., Becker, G.C., Kruse, A., 2019. Experimental and thermodynamic studies of phosphate behavior during the hydrothermal carbonization of sewage sludge. Sci. Total Environ. 692, 147–156. https://doi.org/10.1016/j.scitotenv.2019.07.217.

Palacios, E., Leret, P., De La Mata, M.J., Fernández, J.F., De Aza, A.H., Rodríguez, M.A., 2013. Influence of the pH and ageing time on the acid aluminum phosphate synthesized by precipitation. CrystEngComm 15, 3359–3365. https://doi.org/10.1039/c3ce00011g.

Pradhan, P., Mahajani, S.M., Arora, A., 2018. Production and utilization of fuel pellets from biomass: a review. Fuel Process. Technol. 181, 215–232. https://doi.org/10.1016/j.fuproc.2018.09.021.

Qaramaleki, S.V., Villamil, J.A., Mohedano, A.F., Coronella, C.J., 2020. Factors affecting solubilization of phosphorus and nitrogen through hydrothermal carbonization of animal manure. ACS Sustain. Chem. Eng. 8, 12462–12470. https://doi.org/10.1021/acssuschemeng.0c03268.

Quan, L.M., Kamyab, H., Yuzir, A., Ashokkumar, V., Hosseini, S.E., Balasubramanian, B., Kirpichnikova, I., 2022. Review of the application of gasification and combustion technology and waste-to-energy technologies in sewage sludge treatment. Fuel 316, 123199. https://doi.org/10.1016/J.FUEL.2022.123199.

Reza, M.T., Rottler, E., Herklotz, L., Wirth, B., 2015. Hydrothermal carbonization (HTC) of wheat straw: influence of feedwater pH prepared by acetic acid and potassium hydroxide. Bioresour. Technol. 182, 336–344. https://doi.org/10.1016/j.biortech.2015.02.024.

Rodriguez Correa, C., Bernardo, M., Ribeiro, R.P.P.L., Esteves, I.A.A.C., Kruse, A., 2017. Evaluation of hydrothermal carbonization as a preliminary step for the production of functional materials from biogas digestate. J. Anal. Appl. Pyrolysis 124, 461–474. https://doi.org/10.1016/j.jaap.2017.02.014.

Román, S., Nabais, J.M.V., Laginhas, C., Ledesma, B., González, J.F., 2012. Hydrothermal carbonization as an effective way of densifying the energy content of biomass. Fuel Process. Technol. 103, 78–83. https://doi.org/10.1016/j.fuproc.2011.11.009.

Román, S., Nabais, J.M.V., Ledesma, B., Laginhas, C., Titirici, M.M., 2020. Surface interactions during the removal of emerging contaminants by hydrochar-based adsorbents. Molecules 25. https://doi.org/10.3390/MOLECULES25092264.

Roncal-Herrero, T., Diego, J., Rodriguez-Blanco, R., Benning, L.G., Oelkers, E.H., 2009. Precipitation of iron and aluminum phosphates directly from aqueous solution as a function of temperature from 50 to 200 °C. Cryst. Growth Des. 9, 5197–5205. https://doi.org/10.1021/cg900654m.

Sarrion, A., Diaz, E., de la Rubia, M.A., Mohedano, A.F., 2021. Fate of nutrients during hydrothermal treatment of food waste. Bioresour. Technol. 342, 125954. https://doi.org/10.1016/J.BIORTECH.2021.125954.

Sengupta, S., Nawaz, T., Beaudry, J., 2015. Nitrogen and phosphorus recovery from wastewater. Curr. Pollut. Rep. 1, 155–166. https://doi.org/10.1007/s40726-015-0013-1.

Shaddel, S., Bakhtiary-Davijany, H., Kabbe, C., Dadgar, F., Østerhus, S.W., 2019. Sustainable sewage sludge management: from current practices to emerging nutrient recovery technologies. Sustainability 11. https://doi.org/10.3390/su11123435.

Stratful, I., Scrimshaw, M.D., Lester, J.N., 2001. Conditions influencing the precipitation of magnesium ammonium phosphate. Water Res. 35, 4191–4199. https://doi.org/10.1016/S0043-1354(01)00143-9.

Suarez, E., Tobajas, M., Mohedano, A.F., de la Rubia, M.A., 2022. Energy recovery from food waste and garden and park waste: anaerobic co-digestion versus hydrothermal treatment and anaerobic co-digestion. Chemosphere 297, 134223. https://doi.org/10.1016/J.CHEMOSPHERE.2022.134223.

Szögi, A.A., Vanotti, M.B., Hunt, P.G., 2015. Phosphorus recovery from pig manure solids prior to land application. J. Environ. Manag. 157, 1–7. https://doi.org/10.1016/j.jenvman.2015.04.010.

Vardanyan, A., Kafa, N., Konstantinidis, V., Shin, S.G., Vyrides, I., 2018. Phosphorus dissolution from dewatered anaerobic sludge: effect of pHs, microorganisms, and sequential extraction. Bioresour. Technol. 249, 464–472. https://doi.org/10.1016/J.BIORTECH.2017.09.188.

Villamil, J.A., De La Rubia, M.A., Diaz, E., Mohedano, A.F., 2020a. Technologies for wastewater sludge utilization and energy production: hydrothermal carbonization of lignocellulosic biomass and sewage sludge. Wastewater Treat. Residues as Resour. Biorefinery Prod. Biofuels, pp. 133–153 https://doi.org/10.1016/B978-0-12-816204-0.00007-2.

Villamil, J.A., Mohedano, A.F., San Martín, J., Rodriguez, J.J., de la Rubia, M.A., 2020b. Anaerobic co-digestion of the process water from waste activated sludge hydrothermally treated with primary sewage sludge. A new approach for sewage sludge management. Renew. Energy 146, 435–443. https://doi.org/10.1016/j.renene.2019.06.138.

Wang, Tengfei, Zhai, Y., Zhu, Y., Peng, C., Xu, B., Wang, Tao, Li, C., Zeng, G., 2018. Influence of temperature on nitrogen fate during hydrothermal carbonization of food waste. Bioresour. Technol. 247, 182–189. https://doi.org/10.1016/j.biortech.2017.09.076.

Wang, F., Wang, J., Gu, C., Han, Y., Zan, S., Wu, S., 2019. Effects of process water recirculation on solid and liquid products from hydrothermal carbonization of Laminaria. Bioresour. Technol. 292. https://doi.org/10.1016/J.BIORTECH.2019.121996.

Wang, J., Chen, S., Xu, J.Y., Liu, L.C., Zhou, J.C., Cai, J.J., 2021. High-surface-area porous carbons produced by the mild KOH activation of a chitosan hydrochar and their CO2 capture. New Carbon Mater. 36, 1081–1090. https://doi.org/10.1016/S1872-5805(21)60074-4.

Wang, R., Lei, H., Liu, S., Ye, X., Jia, J., Zhao, Z., 2021. The redistribution and migration mechanism of nitrogen in the hydrothermal co-carbonization process of sewage sludge and lignocellulosic wastes. Sci. Total Environ. 776, 145922. https://doi.org/10.1016/J.SCITOTENV.2021.145922.

Xu, Y., Hu, H., Liu, J., Luo, J., Qian, G., Wang, A., 2015. PH dependent phosphorus release from waste activated sludge: contributions of phosphorus speciation. Chem. Eng. J. 267, 260–265. https://doi.org/10.1016/j.cej.2015.01.037.

Yang, C., Wang, S., Yang, J., Xu, D., Li, Y., Li, J., Zhang, Y., 2020. Hydrothermal liquefaction and gasification of biomass and model compounds: a review. Green Chem. 22, 8210–8232. https://doi.org/10.1039/D0GC02802A.

Yu, Y., Lei, Z., Yang, Xi, Yang, Xiaojing, Huang, W., Shimizu, K., Zhang, Z., 2018. Hydrothermal carbonization of anaerobic granular sludge: effect of process temperature on nutrients availability and energy gain from produced hydrochar. Appl. Energy 229, 88–95. https://doi.org/10.1016/j.apenergy.2018.07.088.

Zhang, T., He, X., Deng, Y., Tsang, D.C.W., Jiang, R., Becker, G.C., Kruse, A., 2020. Phosphorus recovered from digestate by hydrothermal processes with struvite crystallization and its potential as a fertilizer. Sci. Total Environ. 698, 134240. https://doi.org/10.1016/J.SCITOTENV.2019.134240.

Zhou, Y., Shi, W., Engler, N., Nelles, M., 2021. High-value utilization of kitchen waste derived hydrochar in energy storage regulated by circulating process water. Energy Convers. Manag. 229, 113737. https://doi.org/10.1016/J.ENCONMAN.2020.113737.